The 2′-*O*- and 3′-*O*-Cy3-EDA-ATP(ADP) Complexes with Myosin Subfragment-1 are Spectroscopically Distinct

Kazuhiro Oiwa,* David M. Jameson,† John C. Croney,† Colin T. Davis,‡ John F. Eccleston,‡ and Michael Anson‡

*Kanasi Advanced Research Center, Kobe 651-2492, Japan; †Department of Cell and Molecular Biology, John A. Burns School of Medicine, University of Hawaii at Manoa, Honolulu, Hawaii 96822 USA; and ‡National Institute for Medical Research, Mill Hill, London NW7 1AA, UK

ABSTRACT Ribose-modified highly-fluorescent sulfoindocyanine ATP and ADP analogs, 2′(3′)-*O*-Cy3-EDA-AT(D)P, with kinetics similar to AT(D)P, enable myosin and actomyosin ATPase enzymology with single substrate molecules. Stopped-flow studies recording both fluorescence and anisotropy during binding to skeletal muscle myosin subfragment-1 (S1) and subsequent single-turnover decay of steady-state intermediates showed that on complex formation, 2′-*O*- isomer fluorescence quenched by 5%, anisotropy increased from 0.208 to 0.357, and then decayed with turnover rate k_{cat} 0.07 s^{-1}; however, 3′-*O*-isomer fluorescence increased 77%, and anisotropy from 0.202 to 0.389, but k_{cat} was 0.03 s^{-1}. Cy3-EDA-ADP·S1 complexes with vanadate (V_i) were studied kinetically and by time-resolved fluorometry as stable analogs of the steady-state intermediates. Upon formation of the 3′-*O*-Cy3-EDA-ADP·S1·V_i complex fluorescence doubled and anisotropy increased to 0.372; for the 2′-*O*-isomer, anisotropy increased to 0.343 but fluorescence only 6%. Average fluorescent lifetimes of 2′-*O*- and 3′-*O*-Cy3-EDA-ADP·S1·V_i complexes, 0.9 and 1.85 ns, compare with ~0.7 ns for free analogs. Dynamic polarization shows rotational correlation times higher than 100 ns for both Cy3-EDA-ADP·S1·V_i complexes, but the 2′-*O*-isomer only has also a 0.2-ns component. Thus, when bound, 3′-*O*-Cy3-EDA-ADP's fluorescence is twofold brighter with motion more restricted and turnover slower than the 2′-*O*-isomer; these data are relevant for applications of these analogs in single molecule studies.

INTRODUCTION

Single-molecule spectroscopy has become an important method to provide information on the dynamics of complex macromolecules at the level of individual molecules as opposed to ensemble averaging (Lu et al., 1998; Weiss, 1999; Xie and Lu, 1999; Bai et al., 1999; Ha et al., 1999). Fluorescent methods are particularly important in single-molecule enzymology with usually protein and/or substrate (or cofactor) being fluorescent in the visible spectral range. Sulfoindocyanine dyes fluorescent in the red spectrum, such as Cy3 and Cy5 (Mujumdar et al., 1993), are commonly utilized because of their spectral characteristics: Cy3 has a high absorption coefficient of 150,000 M^{-1} cm^{-1} at 549 nm, fluorescence maximum at 570 nm, quantum yield of 0.1−0.5, and exceptional photostability. Myosin Mg-dependent ATPase is the energy-transducing process of muscle intracellular actomyosin-based motility; it was the first enzyme studied using single-substrate molecule techniques by Funatsu et al. (1995) utilizing ATP analogs containing a Cy3 or Cy5 fluorophore attached to the 6-position of the adenine ring with total-internal reflection fluorescence microscopy. However, subsequent work has used ATP modified at the 2′ and 3′ positions of the ribose moiety (Oiwa et al., 1996, 1998, 2000; Eccleston et al., 1996; Jameson and Eccleston, 1997; Iwane et al., 1997; Ishijima et al., 1998; Conibear and Bagshaw, 2000; Kikumoto et al., 2000). Generally, modifications of the ribose moiety have little effect on the interaction of myosin with nucleotide (Tonomura, 1973; Woodward et al., 1991; Oiwa et al., 2000). Such analogs typically exist as an equilibrium mixture of the 2′-*O*- and 3′-*O*-substituted derivatives (Jameson and Eccleston, 1997; Oiwa et al., 2000). However, separated 2′-*O*- and 3′-*O*-Cy3-EDA-ATP isomers exhibit different fluorescent properties both free in solution and on binding to myosin subfragment 1 (S1) (Oiwa et al., 2000): for 2′-*O*-Cy3-EDA-ATP, there is a 12% decrease in fluorescence on binding to S1 with a turnover rate (k_{cat}) of 0.08 s^{-1}, whereas 3′-*O*-Cy3-EDA-ATP, which has 89% fluorescence of the 2′-*O* isomer free in solution, binds to S1 with a 70% increase in fluorescence and k_{cat} 0.022 s^{-1}; 2′-*O*-Cy3-EDA-ADP fluorescence decreases by 5% on binding to S1 compared to an increase of 26% for 3′-*O*-Cy3-EDA-ADP. These differences may reflect changes in the molecular interactions of the two isomers with S1.

To understand the basis of these differences in the fluorescent properties of the two isomers, we have made steady-state and time-resolved fluorescence measurements of intensity and anisotropy on the free nucleotide analogs and their complexes with S1. These measurements were made in a physiological buffer at pH 7.1, 150-mM ionic strength. Initially, we followed the interaction of S1 with the 2′-*O*- and 3′-*O*-EDA-ATP isomers monitoring, in a stopped-flow instrument, time-dependent changes in both intensity and

Submitted March 27, 2002, and accepted for publication August 16, 2002.

Address reprint requests to Michael Anson, National Institute for Medical Research, Mill Hill, London, UK NW7 1AA, UK. Tel.: +44-208-959-3666, ext. 2031; Fax: +44-208-906-4419; E-mail: mike.anson@nimr.mrc.ac.uk.

Abbreviations used: S1, myosin subfragment-1; V_i, vanadate; EDA-ATP, 2′(3′)-*O*-(N-(2-(amino)ethyl)carbamoyl) adenosine triphosphate; 2′)-*O*-Cy3-EDA-AT(D)P, 2′(3′)-*O*-[[2-[[6-[2-[3-(1-ethyl-1,3-dihydro-3,3-dimethyl-5-sulfo-2H-indol-2-ylidene)-1-propenyl]-3,3-dimethyl-5-sulfo-3H-indolio]-1-oxohexyl]amino]ethyl]carbamoyl] adenosine 5′-tri(di)phosphate.

0006-3495/03/01/634/09 $2.00

anisotropy of the nucleotide-protein interactions; thus the formation and decay of the steady-state ATPase reaction intermediates could be observed. We then made similar measurements of a solution of S1 and Cy3-EDA-ATP with excess vanadate (V_i), which leads to the formation of a stable Cy3-EDA-ADP·S1·V_i complex with a half life of ~3 days (Goodno, 1979). This complex is an analog of the transition state between Cy3-EDA-ATP·S1 and Cy3-EDA-ADP·S1·P_i during hydrolysis (Smith and Rayment, 1996; Deng et al., 1998). These data will improve our understanding of intramolecular interactions of 2′-*O*- and 3′-*O*-Cy3-EDA-AT(D)P and intermolecular interaction between these analogs and myosin. These results, some of which have been previously published in preliminary form (Anson et al., 2000, 2002; Oiwa et al., 2001), will be important in both ensemble and single-molecule enzymological investigations of Cy3-nucleotides with myosin II and other motor proteins such as unconventional myosins, kinesins, and dyneins.

MATERIALS AND METHODS

Proteins and nucleotides

Cy3-EDA-ATP and Cy3-EDA-ADP as mixed isomers and their separated 2′-*O*- and 3′-*O*-isomers (Fig. 1 *G*) were prepared and analyzed as described previously (Jameson and Eccleston, 1997; Oiwa et al., 2000). S1 was made from fast-twitch rabbit skeletal muscle myosin by the method of Margossian and Lowey (1982) and its concentration determined optically using A_{280} 0.79 cm^{-1} for 1 mg ml^{-1}. Sodium orthovanadate was prepared as described by Goodno (1979). Cy3·OH was prepared by hydrolysis of its succinimidyl ester (Cy3·OSu, Amersham-Pharmacia Biotech, Amersham, UK) with 50 mM bicarbonate buffer at pH 9.2, and purified using a DE52 ion-exchange column by elution with a linear gradient of 10–200 mM triethylammonium bicarbonate buffer, pH 7.6; HPLC analysis of this material showed ~2% impurity remaining. The free dye was further purified using an HPLC reverse phase column (Nova Pak C18) with isocratic elution by 100 mM triethylamine bicarbonate, pH 7.6, containing 12% acetonitrile (v/v) and monitoring fluorescence (excitation 552 nm, emission 565 nm). Cy3·OH eluted as a single well-resolved peak with <1% impurities. Concentrations of Cy3·OH and the nucleotide analogs were determined using the extinction coefficient 150,000 M^{-1} cm^{-1} at 549 nm. All reagents were of the highest grades commercially available. Nucleotides (and dye) were stored at pH 7 or below and −80°C to minimize isomerization (<1% over several months) and kept on ice directly prior to use.

Fluorescence measurements

All measurements were made at 20°C in pH 7.1 solutions containing 50 mM MOPS/KOH, 100 mM potassium acetate, 5 mM magnesium acetate, 1 mM EGTA, 0.5 mM EDTA, 1 mM potassium phosphate, and 1 mM DTT, having 150 mM ionic strength with 2 mM free Mg^{2+} and <100 nM free Ca^{2+}. Steady-state fluorescence measurements were made using a 10 × 3 mm pathlength fused silica cuvette in an ISS PC1 spectrofluorimeter (ISS, Champaign, IL). Excitation along the 10-mm path was at 514.5 nm, the laser wavelength used for the time-resolved measurements (see below). For anisotropy and total intensity measurements, the exciting light was polarized parallel to the vertical laboratory axis and both the parallel and perpendicularly polarized emission components ($I_\parallel$ and $I_\perp$) were collected through a Schott 087 long-pass (>550 nm) filter. Anisotropy is then given by: $r = (I_\parallel - I_\perp)/(I_\parallel + 2I_\perp)$ and total fluorescence intensity by $f = (I_\parallel + 2I_\perp)$; values were corrected for instrument bias by determining the parallel and perpendicular ratios upon excitation with horizontally polarized light. Stopped-flow fluorescence anisotropy measurements were made with a Hi-Tech Scientific SF 61 instrument (Salisbury, UK) operated in the *T* format and polarization data again collected as described above. Excitation by Hg-Xe lamp was at 540 nm and emission viewed through a Wratten 22 long-pass (>550 nm) filter. All concentrations quoted are those after mixing. Slow kinetics of V_i complex formation were studied using the ISS PC1 spectrofluorimeter.

Analysis of kinetic data

Fluorescence intensity

Time courses of transient fluorescence intensities ($I_\parallel + 2I_\perp$) from kinetic experiments were fitted using a two-step sequential reaction model,

$$\mathrm{A} \xrightarrow{k_1} \mathrm{B} \xrightarrow{k_2} \mathrm{C},$$

where *A* is the initial state, *B* a transient intermediate, and *C* the final state. Observed exponential rate constants, k_1 and k_2, are assumed to be irreversible and first or pseudo-first order. Using the transient concentrations in each state at time *t* as given by Gutfreund (1995) for a fluorophore with initial concentration A_0 and specific fluorescence, F_A, F_B, and F_C, respectively in each of the three states, the total observed fluorescence intensity $f(t)$ is

FIGURE 1 Fluorescence intensity ($I_\parallel + 2I_\perp$) and anisotropy $(I_\parallel - I_\perp)/(I_\parallel + 2I_\perp)$ after stopped-flow mixing 2′-*O*- and 3′-*O*-Cy3-EDA-ATP with excess S1 (*A*, *B*, *C*, *D*) and for V_i complex formation (*E*, *F*). Solutions of 0.5 μM 2′-*O*- or 3′-*O*-Cy3-EDA-ATP and 5 μM S1 (final concentrations in the observation cell) were rapidly mixed and both polarization components $I_\parallel$ and $I_\perp$, recorded with time and converted in *A* and *C* to fluorescence intensity ($I_\parallel + 2I_\perp$), normalized to unity for 0.5 μM free 2′-*O*- or 3′-*O*-Cy3-EDA-ATP, and in *B* and *D* to anisotropy. Double exponential fits using the two-step model (see text) to the data (*black*) are shown (*red* for the 2′-*O* - and *blue* for the 3′-*O*- isomer) with anisotropy fits corrected for fluorescence changes using Eq. 2. In (*A*) for 2′-*O*-isomer (average of five records) the initial rate is 4.0 s^{-1} with steady-state intermediate fluorescence 0.95 and 0.068 s^{-1} final rate; for the 3′-*O*- isomer these are 3.6 s^{-1} and 0.25 s^{-1} with steady-state intermediate fluorescence 1.77 (four records averaged). In (*B*) fits are 3.8 s^{-1} and 0.29 s^{-1} with steady-state intermediate anisotropy 0.357 (2′-*O*- isomer) and 3.8 s^{-1} and 0.25 s^{-1} with anisotropy 0.386 for the 3′-*O*- isomer. Data in *C* and *D* are taken over a longer time scale and show single turnovers. 2′-*O*-Cy3-EDA-ATP turnover (four records averaged) is fitted by exponential rates of 0.067 s^{-1} (−2%) and 0.015 s^{-1} (−1%) in fluorescence (*C*) and 0.29 s^{-1} and 0.094 s^{-1} (31% and 69% amplitude respectively) in anisotropy (*D*). For 3′-*O*-Cy3-EDA-ATP (three records averaged) the fits are 0.25 s^{-1} (−33%) and 0.029 s^{-1} (−67%) in fluorescence (*C*); in anisotropy (*D*), rates are 0.25 s^{-1} and 0.034 s^{-1} (14% and 86% amplitude respectively). In (*E*) total fluorescence intensity and in (*F*) anisotropy changes after addition of 2 mM sodium orthovanadate to a solution of 1 μM subfragment 1 incubated with 0.5 μM 2′-*O*- or 3′-*O*-Cy3-EDA-ATP. The solid lines are best fits of the data by two exponentials using the two-step model: in (*E*) red (2′-*O*-isomer) 0.008 s^{-1} (+3% fluorescence) and 0.0002 s^{-1} (+4%); blue (3′-*O*-isomer) 0.003 s^{-1} (+52% fluorescence) and 0.0005 s^{-1} (+49%). In anisotropy (*F*) equivalent exponential fits (again corrected for fluorescence changes) are: red 0.018 s^{-1} (35% amplitude) and 0.0007 s^{-1} (65%) with final value, 0.329; blue 0.006 s^{-1} (58% amplitude) and 0.0007 s^{-1} (42%) with final value, 0.361. Standard errors are approximately the size of the data symbols and the first data points are ~30 s after V_i addition. All experiments were at pH 7.1, 150 mM ionic strength, and 20°C. (*G*) Shows the structural formulae for 2′-*O*- (1) and 3′-*O*-Cy3-EDA-ATP (2).

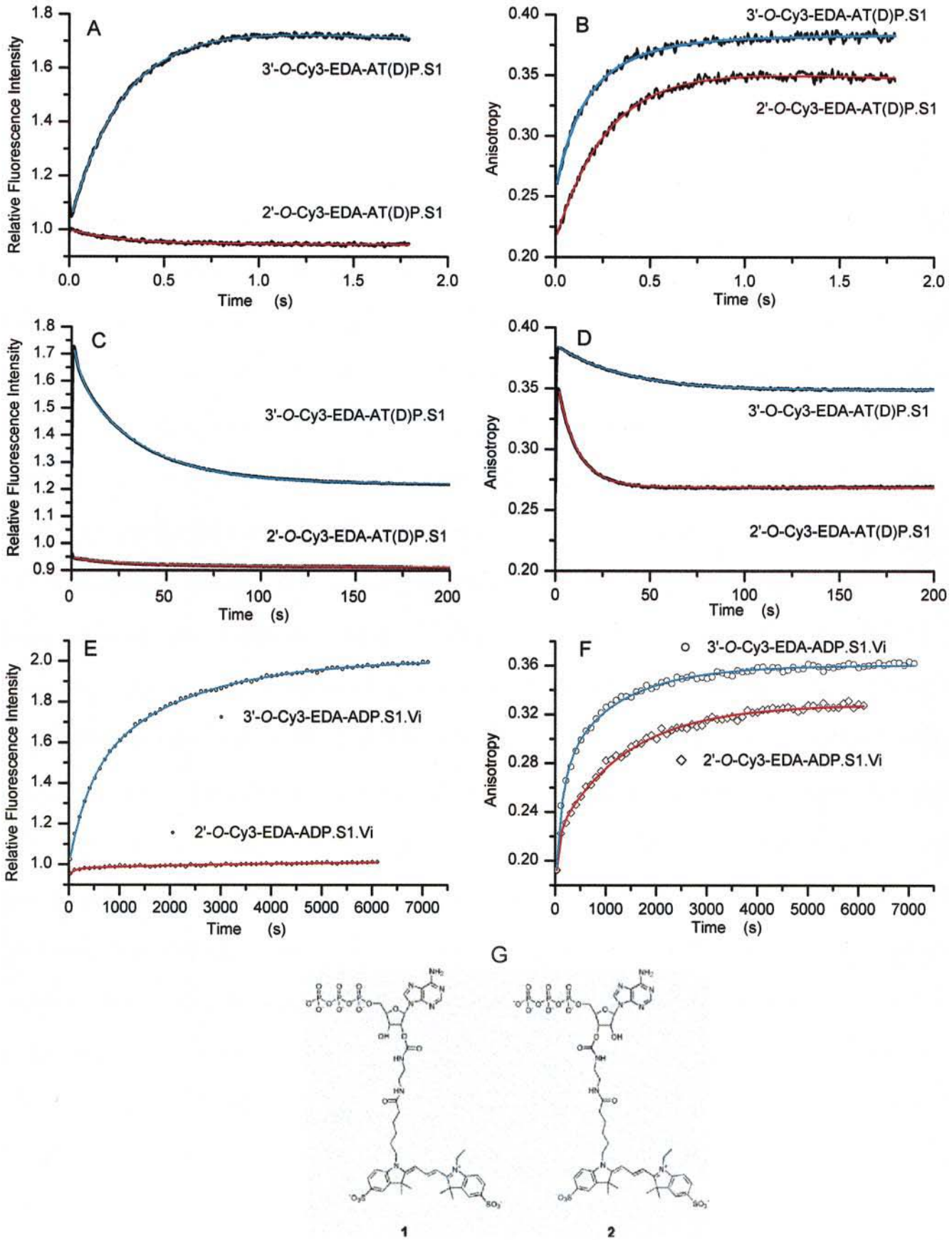
A
Relative Fluorescence Intensity
3'-O-Cy3-EDA-AT(D)P.S1
2'-O-Cy3-EDA-AT(D)P.S1
Time (s)
B
Anisotropy
3'-O-Cy3-EDA-AT(D)P.S1
2'-O-Cy3-EDA-AT(D)P.S1
Time (s)
C
Relative Fluorescence Intensity
3'-O-Cy3-EDA-AT(D)P.S1
2'-O-Cy3-EDA-AT(D)P.S1
Time (s)
D
Anisotropy
3'-O-Cy3-EDA-AT(D)P.S1
2'-O-Cy3-EDA-AT(D)P.S1
Time (s)
E
Relative Fluorescence Intensity
3'-O-Cy3-EDA-ADP.S1.Vi
2'-O-Cy3-EDA-ADP.S1.Vi
Time (s)
F
Anisotropy
3'-O-Cy3-EDA-ADP.S1.Vi
2'-O-Cy3-EDA-ADP.S1.Vi
Time (s)
G
1
2

$$f(t) = A_0(F_A e^{-k_1 t} + F_B k_1 (e^{-k_1 t} - e^{-k_2 t})/(k_2 - k_1) + F_C\{1 - (k_2 e^{-k_1 t} - k_1 e^{-k_2 t})/(k_2 - k_1)\}). \quad (1)$$

Formally, this is identical to fitting by two exponentials with rates k_1 and k_2 and variable relative amplitudes. The apparent turnover rate, k_{cat}, equivalent to the Michaelis-Menten V_{max}, can be calculated (Gutfreund, 1995) as $k_{cat} = k_1 k_2/(k_1 + k_2)$.

Analysis of anisotropy data

Observed anisotropy, $r = (I_\parallel - I_\perp)/(I_\parallel + 2I_\perp)$, is given by the sum of the individual anisotropies weighted by their fraction of the total observed fluorescence intensity (Gutfreund, 1995; Eccleston et al., 2000). For the three-state model with anisotropies r_A, r_B, and r_C, using Eq. 1 this is

$$r(t) = \frac{r_A F_A (k_2 - k_1) e^{-k_1 t} + r_B F_B k_1 (e^{-k_1 t} - e^{-k_2 t}) + r_C F_C (k_2 - k_1 - k_2 e^{-k_1 t} + k_1 e^{-k_2 t})}{F_A (k_2 - k_1) e^{-k_1 t} + F_B k_1 (e^{-k_1 t} - e^{-k_2 t}) + F_C\{k_2 - k_1 - k_2 e^{-k_1 t} + k_1 e^{-k_2 t}\}}. \quad (2)$$

For each experiment the values for specific fluorescence intensities, F_A, F_B, and F_C are determined by fitting data with Eq. 1 and these values are then used to fit the transient anisotropy data using Eq. 2 with r_A, r_B, r_C, k_1, and k_2 set as variable parameters.

Time-resolved fluorometry

Time-resolved fluorescence measurements were made using an ISS K2 multifrequency phase and modulation spectrofluorometer. In this method, the intensity of the exciting 514.5 nm Argon-ion laser emission (Spectra-Physics 2045) is modulated sinusoidally at varying frequencies (typically 1–350 MHz) and the phase shift and relative intensity modulation of the fluorescence determined (Spencer and Weber, 1969). The exciting light is polarized in the vertical laboratory axis and fluorescence viewed through a polarizer oriented at 55° (Spencer and Weber, 1970). Dynamic polarization data are the frequency-domain equivalents to time-decay anisotropy and allow the separation and quantification of rotational modalities in complex systems (Gratton et al., 1984; Jameson and Hazlett, 1991), which were measured with the same instrumentation. All time-resolved measurements were made using the same Schott 087 emission filter used for steady-state fluorimetry.

Phase and modulation data, as functions of modulation frequency were analyzed for lifetimes and anisotropy decay (Jameson et al., 1984; Alcala et al., 1987; Jameson and Hazlett, 1991) using Globals software (Laboratory for Fluorescence Dynamics, University of Illinois at Urbana-Champaign, IL).

RESULTS

Interactions of excess S1 with 2′-*O*- and 3′-*O*-Cy3-EDA-ATP isomers were studied under single turnover conditions by stopped-flow, the instrument being operated with polarizers enabling both fluorescence intensity and anisotropy to be monitored simultaneously. Fig. 1 shows the time courses of initial binding, under pseudo-first-order conditions with 10-fold excess of S1 over Cy3-EDA-ATP, and formation of the steady-state intermediate (Cy3-EDA-ADP·S1·P_i) during a single turnover of each of the two isomers where both fluorescence intensity (normalized to unity for the free Cy3-EDA-ATP analogs) and anisotropy are displayed. With the 3′-isomer there is a 77% increase in fluorescence intensity associated with the steady-state intermediate whereas with the 2′-isomer there is a small (5%) quench (Fig. 1 *A*). The steady-state intermediate fluorescence then slowly decays, after turnover to a mixture of free and bound 2′-*O*- or 3′-*O*-Cy3-EDA-ADP (Fig. 1 *C*). These decays are biphasic and have been analyzed by the two-step model (see Methods and Table 1) with turnover rates (k_{cat}) 0.026 s^{-1} for 3′-*O*-Cy3-EDA-ATP and 0.067 s^{-1} for 2′-*O*-Cy3-EDA-ATP (in the latter case the low value of k_2 (0.015 s^{-1}) for a small (−1%) change in fluorescence is ignored as this may be artifactual due to instrumental drift, photobleaching, or both). A marked difference between the two isomers is evident from the anisotropy data: that of the 2′-isomer on binding to S1 to form the steady-state intermediate increases from 0.208 to 0.357, whereas that of the 3′-isomer increases from 0.202 to 0.389 (Fig. 1 *B*). Anisotropies of the steady-state intermediates of S1 with both isomers then decrease during turnover, but again the final value of the 2′-isomer, 0.269, is lower than that of the 3′-isomer, 0.349 (Fig. 1 *D*). Rates of anisotropy decay are biphasic, with apparent k_{cat} 0.072 s^{-1} for the 2′-isomer and for the 3′-isomer k_{cat} is 0.028 s^{-1}. For details of the kinetics, see Fig. 1 and Table 1.

To elucidate the origins of the differences in fluorescence intensity and anisotropy between 2′-*O*- and 3′-*O*-Cy3-EDA-AT(D)P when bound to S1, one should carry out time-resolved measurements on the steady-state intermediates. However, as described above, these intermediates are only transiently formed, so instead measurements were made on long-lived transition state analogs using solutions of S1 and Cy3-EDA-ATP in the presence of sodium orthovanadate to form the Cy3-EDA-ADP·S1·V_i complex. This complex is stable, unlike the transient complex formed between S1 and Cy3-EDA-ATP. The kinetics of formation of the Cy3-EDA-ADP·S1·V_i complexes were measured to optimize conditions for later measurements.

0.5 μM 2′-*O*- or 3′-*O*-Cy3-EDA-ATP was placed in a fluorescence cuvette at 20°C. S1 was then added to 1 μM and incubated for ~5 min, to effect a single turnover after which Cy3-EDA-ADP·S1 is the predominate bound complex (0.13 μM for K_d = 2.6 μM). Sodium orthovanadate was then added to 2 mM and the time course of the $I_\parallel$ and $I_\perp$ components were recorded. Total fluorescence intensity, again normalized to unity for the free Cy3-EDA-ATP analogs, and anisotropy were computed and these data are also plotted in Fig. 1, *E* and *F*. As shown, the anisotropies of both the 2′-*O*- and 3′-*O*-Cy3-EDA-ADP complexes increased with time. Specifically, the anisotropy of the 2′-*O*-isomer increased from 0.168 to a steady-state value of 0.329 whereas that of the 3′-*O*-isomer increased from 0.170 to

TABLE 1 Transient rates of Cy3-nucleotide.S1 complex formation and turnover at 20°C

Molecular Species	Relative fluorescence ± 0.01 (F_i), F_A, F_B, F_C	Rates from fluorescence intensity (s^{-1}) k_{on}*; k_1; k_2 $k_{cat} = k_1k_2/(k_1 + k_2)$	Anisotropy ± 0.003 (r_i), r_A, r_B, r_C	Rates from anisotropy (s^{-1}) k_{on}*; k_1; k_2 $k_{cat} = k_1k_2/(k_1 + k_2)$
2′-*O*-Cy3-EDA-ADP.S1.P_i	(1)	4.0 ± 0.1*	(0.214)	3.75 ± 0.06*
	0.95	0.067 ± 0.003	0.357	0.29 ± 0.11
	0.93	0.015 ± 0.004	0.331	0.094 ± 0.001
	0.92	[*0.067 ± 0.003*]#	0.269	*0.072 ± 0.007*
3′-*O*-Cy3-EDA-ADP.S1.P_i	(1)	3.53 ± 0.02*	(0.253)	3.80 ± 0.08*
	1.77	0.252 ± 0.006	0.389	0.17 ± 0.09
	1.59	0.029 ± 0.001	0.378	0.0337 ± 0.0002
	1.22	*0.026 ± 0.001*	0.349	*0.028 ± 0.002*
2′-*O*-Cy3-EDA-ADP.S1.V_i	0.95	0.008 ± 0.003	0.168	0.018 ± 0.006
	0.98	0.0002 ± 0.0001	0.224	0.0007 ± 0.00003
	1.02		0.329	
3′-*O*-Cy3-EDA-ADP.S1.V_i	1.00	0.0026 ± 0.0001	0.170	0.006 ± 0.001
	1.52	0.0005 ± 0.00002	0.280	0.0007 ± 0.00005
	2.01		0.361	

F_i is normalized to unity and r_i are starting values determined from fitting stopped-flow data. F_A, F_B, F_C, r_A, r_B, r_C, k_1, and k_2 were determined from fitting data with a two-step first order model (see Methods). Turnover values k_{cat} in *italics* are apparent rates. All data were obtained at 20°C, pH 7.1, and 150-mM ionic strength (see text).

*k_{on} are observed pseudo-first-order rates of initial binding.

#Note that the slow rate is ignored (see text).

0.361. Fluorescence intensity measured over 100 min of the 3′-*O*-isomer increased twofold, but there was only a 7% increase in intensity for the 2′-*O*-isomer.

The time courses of the fluorescence intensity and anisotropy increases could not be well fitted by single exponentials as might be expected inasmuch as the reaction probably involves an initial destabilization of the Cy3-EDA-ADP·S1 complex, followed by rebinding and then by a slow conformational change with a pseudo-first-order rate constant of $1 \times 10^{-2}\ s^{-1}$ (Goodno, 1979). Also, this reaction is not under pseudo-first-order conditions. Fitting by two exponentials with the two-step model (details in Table 1) gave half-times for the 3′-*O*-isomer ~650 s with final fluorescence intensity, 2.01 and in anisotropy, 200 s with final value, 0.361. By comparison, the 2′-isomer gave a small increase in fluorescence intensity (7%) with half-time ~550 s and a corresponding increase in anisotropy to 0.329 with half-time ~440 s. After overnight incubation at 4°C, the steady-state anisotropies of 2′-*O*- and 3′-*O*-Cy3-EDA-ADP·S1·V_i complexes were 0.343 and 0.372, respectively (Table 2), indicating that saturation had not occurred after 7000 s (Fig. 1).

These changes in fluorescence intensities and anisotropies on formation of the Cy3-EDA-ADP·S1·V_i complex are similar to those occurring on formation of the Cy3-EDA-ADP·S1·P_i steady-state intermediate for both isomers. The 3′-isomer gives a large increase in both fluorescence intensity and anisotropy for both complexes whereas the 2′-isomer gives large increases in anisotropy for both complexes accompanied by only small changes in fluorescence intensity. Therefore, Cy3-EDA-ADP·S1·V_i complexes may be used as analogs of Cy3-EDA-ADP·S1·P_i complexes.

In addition to the intensity and anisotropy changes described above, slight changes also occur in the emission maximum of the Cy3 fluorophore on formation of the Cy3-EDA-ADP·S1·V_i complex. Details are given in Table 2 after correction for instrumental response function and polarization. The limiting anisotropy, r_0, was determined from measurements of Cy3·OH dissolved in 99% glycerol. Values of 0.382 at 22°C and 0.386 at −15°C were obtained: this latter value was taken as r_0.

Having established the steady-state properties of the isomers free in solution and bound to S1, we then investigated their time-resolved properties. The multifrequency phase and modulation data for free Cy3·OH, the 2′- and 3′-*O*-Cy3-EDA-ADP isomers, and the 2′- and 3′-*O*-Cy3-EDA-ADP·S1·V_i complexes are shown in Fig. 2. In no

TABLE 2 Average lifetimes, emission maxima, and steady-state anisotropies of Cy3 nucleotides measured at 20°C, pH 7.1

Molecular species	Average lifetime $\langle\tau\rangle$ ns ± 10%	λ_{max} nm ± 0.5	Steady-state anisotropy ± 0.003
Cy3·OH (99% glycerol at −15°C)		566.0	0.386*
Cy3·OH	0.20	562.0	0.334
2′-O-Cy3-EDA-ATP	0.68	563.5	0.208
3′-O-Cy3-EDA-ATP	0.72	563.5	0.202
2′-O-Cy3-EDA-ADP	0.72	563.5	0.195
3′-O-Cy3-EDA-ADP	0.55	563.5	0.225
2′-O-Cy3-EDA-ADP·S1·V_i	0.90	565.0	0.343
3 3′-O-Cy3-EDA-ADP·S1·V_i	1.85	562.0	0.372

Note that the high anisotropies observed for the free dye and nucleotides in solution reflect their short fluorescent lifetimes.

*This value is taken as r_0, the limiting anisotropy.

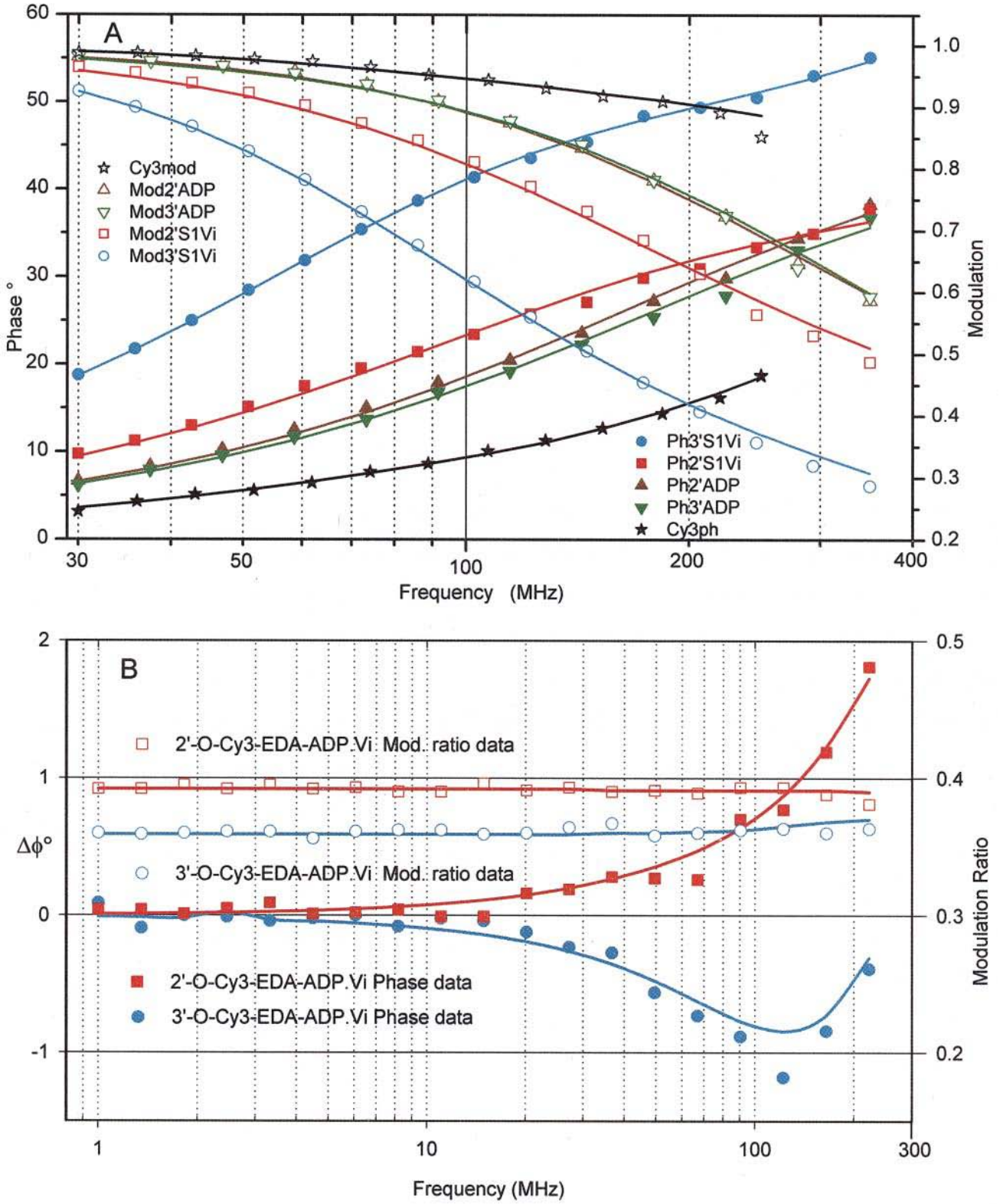

FIGURE 2 (*A*) Multifrequency phase and modulation data for Cy3-OH, 2′-*O*- and 3′-*O*-Cy3-EDA-ATP and −ADP free in solution and bound to S1 as the Cy3-EDA-ADP·S1·V_i complexes. The open symbols are the modulation data and the solid symbols are the phase data, determined at 20°C in the same buffer as for Fig. 1. The lines represent the best fits to combined phase and modulation data, with average fluorescence lifetimes as recorded in Table 2. (*B*) Dynamic polarization data for 2′-*O*- and 3′-*O*-Cy3-EDA-ADP·S1·V_i complexes. Solid symbols correspond to ΔΦ data (the phase delay between the perpendicular and parallel components) whereas open symbols correspond to the modulation ratio (the ratio perpendicular/parallel of the AC components). 2′-*O*-isomer data are indicated by squares and 3′-*O*- isomer data by circles, and were measured under the same conditions as for Fig. 2 *A*. The actual fits (*red line* for 2′-*O*-isomer

case could the fluorescence intensity decay data be well fit by a single exponential (apart from free Cy3-OH, see below), but were better fit by either sums of exponentials or distribution functions (Jameson and Hazlett, 1991): the fitted values presented in Fig. 2 represent average lifetimes $< \tau >$, calculated as: $< \tau > = \Sigma f_i \tau_i$, where f_i represents the fractional contribution to the total intensity and τ_i the lifetime respectively of the *ith* component—discrete exponential decays (either two or three components) being used to generate average lifetime values. Raw phase and modulation data show that the average lifetimes for these fluorescent species fall into the sequence: Cy3·OH < 2′ (3′)-*O*-Cy3-EDA-ATP, 2′-*O*-Cy3-EDA-ADP·S1·V_i < 3′-*O*-Cy3-EDA-ADP·S1·V_i (see Table 2). The lifetime of Cy3·OH in aqueous solution was essentially monoexponential, being dominated (~99%) by a very short component, 0.20 ± 0.05 ns, and only a very small amount (~1%) of a longer component near 1.5 ns. The long component could correspond to an impurity in the sample (we note that the fractional contribution of this component to the fluorescence was originally ~4% but decreased to the final value of ~1% after HPLC purification). The average lifetimes of both 2′-*O*- and 3′-*O*-Cy3-EDA-ADP and ATP isomers were longer than that of the free Cy3·OH but the lifetime decays in these cases were not monoexponential. The precision of the data was not considered sufficient to determine the detailed exponential decay characteristics but the average values for three of the free fluorescent nucleotide analogs (as shown in Table 2) are similar. The average lifetime of the 3′-*O*-Cy3-EDA-ADP analog was slightly shorter than the other three nucleotide analogs which could account for the slightly higher anisotropy associated with this analog (Table 2). When complexed with S1 the two isomers exhibited distinctly different excited state properties from each other and from the free analogs. Again, in these cases the lifetime decays were not monoexponential but were better fit by either sums of discrete exponentials or distribution functions. The average lifetimes associated with the 2′- and 3′-*O*- bound ADP analogs were 0.90 and 1.85 ns, respectively (Table 2). In both cases the component lifetimes consisted of a longer component (1.48 ns in the case of the 2′-*O*-isomer and 2.28 ns in the case of the 3′-*O*-isomer) along with shorter components that may arise, in part, due to small contributions from unbound analogs: these have been assimilated into the average lifetimes in Table 1. The dynamic polarization (time-decay anisotropy) data associated with the 2′-*O*- and 3′-*O*-Cy3-EDA-ADP·S1·V_i complexes are also shown in Fig. 2. The negative $\Delta\phi$ values observed for the 3′-*O*-isomer show an anomalous phase delay, also known as a "Chip Dip" (Hazlett et al., 1989; Jameson and Hazlett, 1991), which is due to a small amount of free, i.e., unbound, nucleotide analog. From the lifetimes (assuming lifetimes and quantum yields are proportional) and fractional intensities attributed to free and bound 3′-*O*-EDA-ADP, the concentration of free 3′-*O*-Cy3-EDA-ADP can be estimated as $\sim 10^{-7}$ M consistent with a dissociation constant of $\sim 10^{-7}$ M for the nucleotide/myosin vanadate complex. Taking this free nucleotide into account, the fluorescent moiety in the 3′-*O*-Cy3-EDA-ADP·S1·V_i complex does not display any significant mobility during the excited state lifetime; i.e., all the observed anisotropy decay was associated with a very slow rotational component (>100 ns rotational correlation time). In contrast, the fluorescent moiety in the 2′-*O*-Cy3-EDA-ADP·S1·V_i complex exhibited two rotational motions. In this case also, data were consistent with ~100 nM unbound nucleotide but were only fit well by a model having two rotational components for the bound probe. The major rotational component was, as for the 3′-*O*-isomer, very slow (>100 ns rotational correlation time) but the minor rotational component (~10% of the observed anisotropy decay) was associated with a fast component (~0.2 ns rotational correlation time).

DISCUSSION

The complexes of the 2′-*O*- and 3′-*O*-isomers of Cy3-EDA-ATP with S1 could not be studied directly by time-resolved fluorescence methods because of their transient nature. Kinetic studies (Goodno, 1979; Goodno and Taylor, 1981) showed the Mg·ADP·S1·V_i stable complex to be a good analog of the Mg·ADP·S1·P_i steady-state intermediate after ATP hydrolysis. Subsequent high resolution structural studies in crystals (Smith and Rayment, 1996) and in solution by Raman spectroscopy (Deng, et al., 1998) have shown that the V_i complex rather mimics the transition state during Mg-dependent ATP hydrolysis. However, the structural differences between these two complexes are probably minor and relate mainly to the presence of the nucleophilic water molecule that attacks the γ-phosphate of Mg·ATP during hydrolysis.

First, we examined the interaction of S1 with 2′-*O*- and 3′-*O*-Cy3-EDA-ATP to characterize their steady-state intermediates under the conditions used in subsequent experiments. The buffer employed was chosen to mimic muscle cell physiological conditions. Fluorescence intensity and anisotropy measurements were made, both in stopped-flow

and *blue* for 3′-*O*-isomer) correspond to limiting anisotropies (r_0) of 0.385 in both cases with a rotational correlation time of 0.75 ns for both free Cy3-EDA-ADPs, and fractional contributions to the intensities of 0.064 and 0.049, with lifetimes of 0.55 ns and 0.72 ns for free 3′-*O*- and 2′-*O*-isomers, respectively. For the bound nucleotide analogs, lifetimes of 2.28 ns and 1.48 ns for the 3′-*O*- and 2′-*O*-isomers, respectively, were used. The fit to the 3′-*O*- isomer data could not be improved by including a second rotational component for the bound nucleotide: the single rotational component found was ~500 ns, too long to resolve with precision, given the short lifetime of the bound nucleotide. In the case of the 2′-*O*-isomer, the fit required a second rotational correlation time of 0.20 ns for the bound nucleotide, with a fractional contribution of 10%; the long rotational correlation time was ~200 ns, also too long to resolve with precision.

and steady-state fluorimetry. These changes in solution conditions, optics, and measurement technique may all contribute to differences between data reported here and in Oiwa et al. (2000). The fluorescence increase and turnover rate (k_{cat}) seen on binding 3′-*O*-Cy3-EDA-ATP to S1 are similar to those seen previously (+77% and 0.026 s^{-1} compared to +70% and 0.022 s^{-1}). However, for 2′-*O*-Cy3-EDA-ATP binding to S1, these are slightly different (−5% and 0.067 s^{-1} compared to −12% and 0.080 s^{-1}). Anisotropy measurements of the decay of the steady-state intermediates (Cy3-EDA-ADP·S1·P_i) show differences between the two isomers, although their free anisotropies are similar, at 0.208 and 0.202, respectively. Turnover rates determined from anisotropy and fluorescence intensity are similar for each isomer although the fluorescence change for the 2′-*O*-isomer is small. Again, the 2′-*O*-isomer shows ~2.5-fold faster turnover than the 3′-*O*-isomer; this compares with 3.5-fold seen by Oiwa et al. (2000).

As the kinetics were in all cases biphasic and could not be well described by single exponentials, we have applied the double first-order exponential decays predicted by the simple two-step model as described by Gutfreund (1995). We have adapted this model, which has the virtue of being essentially the simplest description of a biphasic process, to describe anisotropy decay as well; the complexity of Eq. 2 merely reflects the effects of fluorescence changes on the anisotropy kinetics.

The steady-state fluorescence properties of the V_i complexes of Cy3-EDA-ADP with S1 (Fig. 2) show some differences between those of the steady-state intermediates, as may be expected inasmuch as they actually mimic the transition state during ATP hydrolysis (see the discussion above). For the 2′-*O*-isomer on formation of the V_i complex there was a 7% increase in fluorescence intensity compared to a 5% decrease for the steady-state intermediate; in anisotropy much larger changes were recorded, from 0.168 to an equilibrium value of 0.343 compared to 0.364 for the steady-state intermediate. For the 3′-*O*- isomer a 2.0-fold increase in fluorescence intensity was seen accompanied by an anisotropy change from 0.187 to 0.372 on formation of the V_i complex compared with a 1.77-fold fluorescence intensity change and anisotropy increase to 0.389 for the steady-state intermediate. It should be noted that the low starting anisotropies for the V_i complex formation may imply an initial destabilization of the Cy3-EDA-ADP·S1 complex on adding vanadate as suggested by Goodno (1979). Further, the anisotropies of the steady-state intermediates are similar to the r_0, 0.386, determined for the Cy3·OH fluorophore alone. The stability of the fluorescence and anisotropy of the two V_i complexes during such long observation periods supports the implicit assumption that the isomerization between the 2′-*O*- and 3′-*O*- isomers is negligible during these experiments. A half-life for such isomerization of >3 days at 20°C was reported in Oiwa et al. (2000) which is comparable to the V_i complex half-life of ~3 days (Goodno, 1979). Therefore, although there are differences in the fluorescence intensity and anisotropy changes between the two isomers on forming the two complexes, the differences between their respective steady-state P_i intermediates and the corresponding stable V_i complexes are minor even though they were measured with different instruments, and so suggest that data from the V_i complex can be related to our present and previous studies on the interaction of the Cy3-EDA-AT(D)P isomers with S1 (Oiwa et al., 2000).

The average fluorescence lifetime values summarized in Table 2, as discussed in the Results section, indicate complexity in all of the systems studied. In the case of the 2′-*O*- and 3′-*O*-isomers of Cy3-EDA-AT(D)P the lifetime values may be influenced by intramolecular quenching of the fluorescent moiety by the nucleotide moiety but further studies must be carried out to clarify the molecular interactions involved. When bound to S1 it is clear that environments of the fluorescent moieties in each case are different. It is probable that the longer lifetime of the 3′-*O*-isomer complex is related to a more restricted mobility. For example, it may be that this limited mobility prevents the fluorescent moiety in this case from contact with a quenching group (either a water molecule, or an amino acid residue) which the more mobile and more quenched 2′-*O*-isomer encounters. Another possibility is that the conformational state of the 3′-*O*-isomer excludes more solvent than that of the 2′-*O*-isomer. The time-resolved anisotropy results would seem to support these hypotheses inasmuch as the 2′-*O*-isomer has a fast rotational component at 0.2 ns in addition to the slow rotational correlation time of >100 ns shown by both isomers. More detailed analysis of the mobility of the fluorophore in the complexes requires accurate knowledge of free nucleotide analog concentrations in equilibrium with Cy3-EDA-ADP·S1·V_i complexes, entailing measurements at different concentrations and determination of the S1's enzymatic activity; this is outside the scope of the present work.

An alternative mechanism has been postulated for the increases in fluorescence observed for these sulfoindocyanine dyes on binding to macromolecules or surfaces by Luby-Phelps et al. (1988): increased rigidity of the environment reduces the torsional motion of the conjugated ring structures, thereby better maintaining a planar fluorophore and so enhancing quantum yield.

If it be assumed that fluorescent quantum yields are proportional to the lifetimes determined here and that free Cy3·OH has a value of 0.04 (Mujumdar et al., 1993), then both free 2′-and 3′-*O*-Cy3-EDA-ATP will have apparent quantum yields of ~0.14 but when bound to S1 that of the 2′- isomer will increase to 0.18 whereas for the 3′- isomer the quantum yield will increase to 0.37. We have shown here in ensemble experiments that there will be a twofold enhancement of fluorescence for the binding of 3′-*O*-Cy3-EDA-ATP to S1 compared to the 2′- isomer with similar binding kinetics but different hydrolysis rates, emphasizing the need to utilize pure isomers of nucleotide analogs. It has

been shown that the stable complexes of 2′- and 3′-*O*-Cy3-EDA-ADP bound to S1 with V_i are good analogs of the steady-state intermediates seen during Mg·ATP hydrolysis and so could be applied to further studies of the myosin triphosphatase and coupled mechanical mechanisms at the level of single molecules. Finally, the anisotropy results clearly demonstrate that in the case of probes such as 2′-*O*-Cy3-EDA-AT(D)P, very small changes in fluorescence intensity may be accompanied by large changes in anisotropy such that observation of this parameter would facilitate measurement in both ensemble and single molecule enzymology.

We thank Dr. D. R. Trentham for helpful discussion of this work.

K.O. gratefully acknowledges support from a Grant in Aid from the Japan Ministry of Education, Science, and Culture. D.M.J. acknowledges support from the National Science Foundation (Grant MCB9808427) and from the American Heart Association (Grant 9950020N). M.A. is grateful to the British Council for travel support.

REFERENCES

Alcala, J. R., E. Gratton, and F. G. Prendergast. 1987. Fluorescence lifetime distributions in proteins. *Biophys. J.* 51:597–604.

Anson, M., K. Oiwa, J. F. Eccleston, and D. M. Jameson. 2000. Fluorescence lifetime and polarization measurements by phase fluorometry of 2′-O- and O-Cy3-EDA-ATP(ADP) on binding to myosin subfragment-1. *Biophys. J.* 78:A753. (Abstr.)

Anson, M., J. F. Eccleston, K. Oiwa, J. C. Croney, and D. M. Jameson. 2002. Transient anisotropy and lifetime studies of 2′ and 3′-*O*-Cy3-EDA-AT(D)P complexes with myosin-S1. *Biophys. J.* 82:436A. (Abstr.)

Bai, C., C. Wang, X. S. Xie, and P. G. Wolynes. 1999. Single molecule physics and chemistry. *Proc. Natl. Acad. Sci. USA*. 96:11075–11076.

Conibear, P. B., and C. R. Bagshaw. 2000. A comparison of optical geometries for combined flash photolysis and total internal reflection fluorescence microscopy. *J. Microsc.* 200:218–229.

Deng, H., J. Wang, R. H. Callender, J. C. Grammer, and R. G. Yount. 1998. Raman difference spectroscopic studies of the myosin S1.MgADP.vanadate complex. *Biochemistry*. 37:10972–10979.

Eccleston, J. F., K. Oiwa, M. A. Ferenczi, M. Anson, J. E. T. Corrie, A. Yamada, H. Nakayama, and D. R. Trentham. 1996. Ribose-linked Sulfoindocyanine Conjugates of Cy3-EDA-ATP and Cy5-EDA-ATP. *Biophys. J.* 70:A159. (Abstr.)

Eccleston, J. F., J. P. Hutchinson, and H. D. White. 2000. Stopped flow techniques. *In* Protein Ligand Interactions: Structure and Spectroscopy. A Practical Approach Series. S. E. Harding and B. Z. Chowdhry, editors. Oxford University Press, Oxford, UK.

Funatsu, T., Y. Harada, M. Tokunaga, K. Saito, and T. Yanagida. 1995. Imaging of single fluorescent molecules and individual ATP turnovers by single myosin molecules in aqueous solution. *Nature*. 374:555–559.

Goodno, C. C. 1979. Inhibition of myosin ATPase by vanadate ion. *Proc. Natl. Acad. Sci. USA*. 76:2620–2624.

Goodno, C. C., and E. W. Taylor. 1981. Inhibition of actomyosin ATPase by vanadate. *Proc. Natl. Acad. Sci. USA*. 79:21–25.

Gratton, E., D. M. Jameson, and R. D. Hall. 1984. Multifrequency phase and modulation fluorometry. *Annu. Rev. Biophys. Bioeng*. 13:105–124.

Gutfreund, H. 1995. Kinetics for the Life Sciences. Cambridge University Press, Cambridge, UK.

Ha, T., A. Y. Ting, J. Liang, W. B. Caldwell, A. A. Deniz, D. S. Chemla, P. G. Schultz, and S. Weiss. 1999. Single-molecule fluorescence spectroscopy of enzyme conformational dynamics and cleavage mechanism. *Proc. Natl. Acad. Sci. USA*. 96:893–898.

Hazlett, T. L., A. E. Johnson, and D. M. Jameson. 1989. Time-resolved fluorescence studies on the ternary complex formed between bacterial elongation factor Tu, guanosine 5′-triphosphate, and phenylalanyl-tRNAPhe. *Biochemistry*. 28:4109–4117.

Ishijima, A., H. Kojima, T. Funatsu, M. Tokunaga, H. Higuchi, H. Tanaka, and T. Yanagida. 1998. Simultaneous observation of individual ATPase and mechanical events by a single myosin molecule during interaction with actin. *Cell*. 92:161–171.

Iwane, A. H., T. Funatsu, Y. Harada, M. Tokunaga, O. Ohara, S. Morimoto, and T. Yanagida. 1997. Single molecular assay of individual ATP turnover by a myosin-GFP fusion protein expressed in vitro. *FEBS Lett*. 407:235–238.

Jameson, D. M., and J. F. Eccleston. 1997. Fluorescent nucleotide analogs: synthesis and applications. *Meth. Enzymol*. 278:363–390.

Jameson, D. M., E. Gratton, and R. D. Hall. 1984. The measurement and analysis of heterogeneous emissions by multifrequency. *Appl. Spectro. Rev*. 20:55–106.

Jameson, D. M., and T. L. Hazlett. 1991. Time-resolved fluorescence measurements in biology and biochemistry. *In* Biophysical and Biochemical Aspects of Fluorescence. G. Dewey, editor. Plenum Press, New York. 105– 133.

Kikumoto, M., K. Oiwa, and M. Anson. 2000. Single molecule kinetic studies using fluorescent ATP analogs: photobleaching and myosin ATPase rates of Alexa546-, Alexa532- and Cy3-EDA-ATP. *Biophys. J.* 78:385A. (Abstr.)

Lu, H. P., L. Xun, and X. S. Xie. 1998. Single-molecule enzymatic dynamics. *Science*. 282:1877–1882.

Luby-Phelps, K., K. A. Guss, L. Ernst, R. B. Mujumdar, S. R. Mujumdar, and A. S. Waggoner. 1988. The solvent viscosity of the cytomatrix as measured by ratio imaging. *J. Cell Biol*. 107(Suppl.):15a (Abstr.).

Margossian, S. S., and S. Lowey. 1982. Preparation of myosin and its subfragments from rabbit skeletal muscle. *Meth. Enzymol*. 85:55–71.

Mujumdar, R. B., L. A. Ernst, S. R. Mujumdar, C. J. Lewis, and A. S. Waggoner. 1993. Cyanine dye labeling reagents: sulfoindocyanine succinimidyl esters. *Bioconjug. Chem*. 4:105–111.

Oiwa, K., M. Anson, J. F. Eccleston, J. E. T. Corrie, A. Yamada, H. Nakayama, and D. R. Trentham. 1996. Microscopic observations of single Cy3-EDA-Adenine nucleotide molecules interacting with myosin filaments in vitro. *Biophys. J.* 70:A159. (Abstr.)

Oiwa, K., M. Anson, J. F. Eccleston, and D. R. Trentham. 1998. Isolation and characterization of 2′-*O*- and 3′-*O*- isomers of Cy3-EDA-ATP: kinetics and single molecule studies. *Biophys. J.* 74:A260. (Abstr.)

Oiwa, K., J. F. Eccleston, M. Anson, M. Kikumoto, C. T. Davis, G. P. Reid, M. A. Ferenczi, J. E. T. Corrie, A. Yamada, H. Nakayama, and D. R. Trentham. 2000. Comparative single-molecule and ensemble myosin enzymology: sulfoindocyanine ATP and ADP derivatives. *Biophys. J.* 78:3048–3071.

Oiwa, K., D. M. Jameson, J. C. Croney, J. F. Eccleston, and M. Anson. 2001. Fluorescence, anisotropy and lifetime measurements of 2′ and 3′-O-Cy3-EDA-A(T)DP binding in myosin-S1. Vanadate complexes. *Biophys. J.* 80:A1401. (Abstr.)

Smith, C. A., and I. Rayment. 1996. X-ray structure of the magnesium(II)·ADP·vanadate complex of the *Dictyostelium discoideum* myosin motor domain to 1.9 A resolution. *Biochemistry*. 35:5404–5417.

Spencer, R. D., and G. Weber. 1969. Measurement of subnanosecond fluorescence lifetimes with a cross-correlation phase fluorometer. *Ann. N. Y. Acad. Sci.* 158:361–376.

Spencer, R. D., and G. Weber. 1970. Influence of Brownian rotations and energy transfer upon the measurements of fluorescence lifetime. *J. Phys. Chem*. 52:1654–1663.

Tonomura, Y. 1973. ATP analogues. *In* Muscle Proteins, Muscle Contraction and Cation Transport. University Park Press, Tokyo, Japan. 257–271.

Weiss, S. 1999. Fluorescence spectroscopy of single biomolecules. *Science*. 283:1676–1683.

Woodward, S. K. A., J. F. Eccleston, and M. A. Geeves. 1991. Kinetics of the interaction of 2′(3′)- *O*-(*N*-methylanthraniloyl)-ATP with myosin subfragment 1 and actomyosin subfragment 1: characterization of two acto-S1-ADP complexes. *Biochemistry*. 30:422–430.

Xie, X. S., and H. P. Lu. 1999. Single-molecule enzymology. *J. Biol. Chem*. 274:15967–15970.